Machine Learning Model for Surface Finish in Ultra-Precision Diamond Turning

N. E. Sizemore
Department of Mechanical Engineering
UNC Charlotte
Charlotte, NC, USA

M. L. Nogueira
Poole College of Management
North Carolina State University
Raleigh, NC, USA

N. P. Greis
Poole College of Management
North Carolina State University
Raleigh, NC, USA

T. L. Schmitz
Department of Mechanical Engineering
UNC Charlotte
Charlotte, NC, USA

M. A. Davies
Department of Mechanical Engineering
UNC Charlotte
Charlotte, NC, USA

ABSTRACT
In diamond machining freeform and symmetric optics, it is essential to ensure that surface characteristics are maintained. Optics for imaging applications require tight tolerances on surface roughness, mid-spatial frequencies, and form. This work predicts surface roughness in diamond turning as a function of machining parameters using machine learning. Diamond turning is chosen for its relative simplicity when compared to other machining operations. No tool wear is expected, and the surface is generated by a simple geometric replication of the tool into the surface for a wide range of parameters. Machine learning algorithms are trained by associating machining characteristics / parameters with the resulting surface finish performance measures. Surface finish prediction results obtained with traditional regression machine learning algorithms are reported, including a general regression neural network. Work is ongoing to further validate results and use additional diamond turning machining data to train the neural network. In addition, work continues to better interpret the effects of machining parameters on the surface function estimates obtained by the machine learning algorithms.

INTRODUCTION
In manufacturing of optics, research institutes and industries alike are making use of ultra-precision manufacturing techniques to produce high quality optics and optical mold surfaces [1]. Techniques such as single point diamond turning on an ultra-precision machine tool can be employed to manufacture precision, rotationally symmetric optics with optical quality surface roughness and form [3]. In the past decade, optics manufacturing has become increasingly challenging with the implementation of freeform optics [3]. The major benefits of freeform surfaces are the reduction of components necessary in a product and the ability to contain multiple reflective or diffractive functions in a single optic. Freeform surfaces can be described as asymmetric, or lacking a single axis of rotation about which symmetry can be defined. These complex geometries require the use of multi-axis (>2) ultra-precision machine tools; the associated sub-aperture manufacturing techniques introduce new challenges not encountered in traditional diamond turning.

For both freeform and symmetric optics, maintaining the key surface characteristics is of critical importance. Optics for imaging applications, including telescopes, spectrometers, energy concentrators, and thermal imaging optics, require tight tolerances on surface roughness, mid-spatial frequencies, and form that are related to the wavelength of light in a particular application. Suleski et al. showed the degrading effect on imaging quality of raster milled versus turned surfaces for visible light applications [4]. Another example includes high-powered

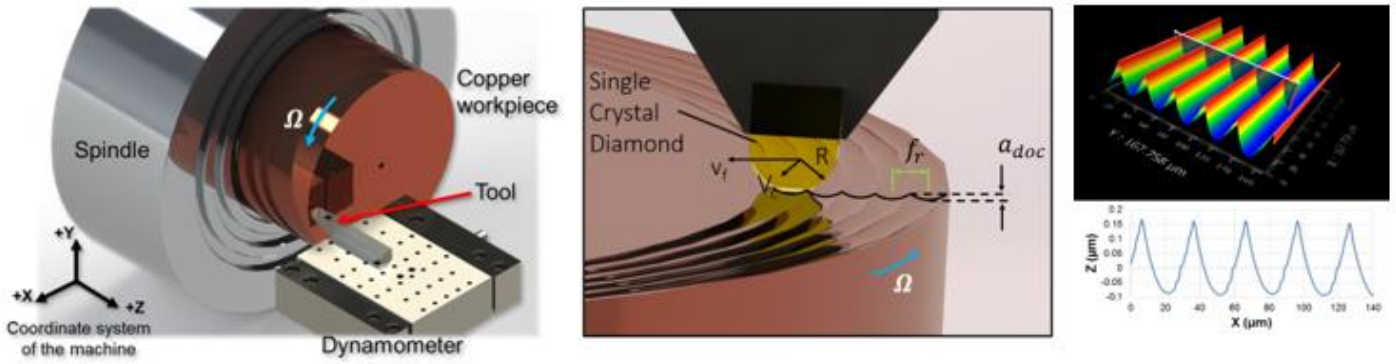

(a) (b) (c)

Figure 1: (a) Diamond turning arrangement; (b) diamond turning parameter definitions; and (c) measurement of typical diamond turned surface under ideal cutting conditions.

laser applications that use reflective optics manufactured from oxygen-free high-conductivity (OFHC) copper [2]. Surface finish, or roughness, is crucial in laser applications due to the effect of light scatter [5,6] and subsurface defects that act as energy concentrators. These cause heat spikes in the material which can degrade the surface and subsurface over time [7].

In diamond machining, key process signatures can be directly detected in the machined specimen surface. In traditional diamond machining, an extremely sharp (~100 nm edge radius) round-nosed tool cuts a surface, leaving circular cusp structures by direct geometric replication of the tool shape into the diamond turned surface (see Figure 1(c)). However, geometric replication of the tool is a very simplified description of the process. Diamond machining involves complex, high-strain rate material flow and the physics of this flow can affect surface structure. In addition, the tool is not infinitely stiff. Deflections and dynamics from the machine tool or cutter interacting with the workpiece will result in lower quality surfaces. Further, dimensional changes occur due to temperature variations. In cutting complex freeform optics, for example, cycling of the machine chillers have been observed to add other more slowly varying time fluctuations that can translate into surface structures at various length scales. These undesired effects drive manufacturers to employ more conservative machining parameters which results in longer machine times and higher costs. Because the surface characteristics result from such a complex interaction of machining parameters, they have not been fully captured by existing physics-based models. Thus, the goal of this work is to develop a machine learning model for the prediction of surface quality in diamond turning as a function of machining parameters, with the end goal of providing manufacturers with a tool for optimizing the processes and reducing costs.

Until recently, statistical methods including regression, ANOVA, and the Taguchi method among others, have guided the search for models that capture the relationship between surface roughness and the optimal cutting parameters that achieve the desired surface roughness [8-16]. As noted, the complex interaction of machining parameters contributes to model error, which can lead to disagreement between the surface finish predictions from data-learning models and (admittedly incomplete) physics-based models. Machining relationships, in addition, are highly nonlinear requiring simplifying assumptions in the physics-based models that compromise predictive performance; in fact, existing physics-based models are used mostly for guidance and not for prediction. Data learning models, on the other hand, have demonstrated higher accuracy in surface roughness prediction and associated optimal cutting parameters due to their ability to represent both linear and nonlinear relationships among and between cutting parameters, and to learn these relationships directly from experimental data. In additional to their predictive capability, data learning models can identify unexpected dependencies between surface finish results and parameters that suggest new physical models.

While there has been a great deal of work predicting surface finish in complex machining operations where many physical phenomena including tool wear and complex material flow are operative [8-9,11], the focus of this paper is a more tractable problem, the prediction of surface roughness in diamond turning of OFHC copper. For a large range of parameter values, the surface generation in the turning of OFHC copper can be approximated by a pure geometric replication of the round tool nose into the material surface. Under these conditions, the roughness is dominated by two machining parameters. However, for other ranges of parameters, the surface

finish is dependent on more complex chip formation processes and machining parameters that relate to other physical effects, such as material behavior, tool vibration, and short-term thermal fluctuations. The logic of the approach is to provide a training set that will enable the machine learning model to identify a known physical model for some parameter ranges while providing new physical insights for observed behavior over other ranges of parameters.

EXPERIMENTAL ARRANGEMENT

The simplified diamond turning experiment is described in Figure 1. A single crystal diamond tool generates a nominally planar cusped surface on a rotating copper workpiece as shown in Figure 1(a). The tool is mounted on a dynamometer to measure cutting forces; however, for simplicity, force data is not used here. The input parameters for the machine learning models are illustrated in Figure 1(b) and summarized in Table 1: spindle speed or rotation rate Ω, in rev/min (rpm), tool nose radius R, in μm, rake angle α, in degrees[a], cutting speed V_c, in m/s, feed velocity V_f, in mm/min, axial depth of cut a_{doc}[b], in μm, and feed per revolution f_r[c], in μm/rev. Figure 1(c) shows an example surface measurement from a coherence scanning interferometer (CSI), and a cross section of the surface demonstrating the geometric replication of the tool geometry into the surface. Under ideal conditions, there is a cusp structure with spacing f_r and radius R. This cusp structure dominates the surface micro-roughness.

Table 1: Parameter ranges

R (μm)	α (deg)	V_c (m/sec)	f_r (μm/rev)	a_{doc} (μm)
250	0	3	{0.1; 0.3; 1.0; 2.0; 5.0; 10; 20; 30; 40}	{1.0; 10}
250	0	0.3	{0.1; 0.3; 1.0; 2.0; 5.0; 10; 20; 30; 40}	{1.0; 10}

There are many mathematical parameters used to quantify surface roughness (e.g. Sq, aerial root-mean-square, Sz, areal peak to valley, etc.). Here the arithmetic mean surface roughness Sa is applied, which, for geometric replication, has a simple analytical relationship to the machining parameters.

$$Sa \cong \frac{f_r^2}{9\sqrt{12}R} \quad (Eq.1)$$

Based on the geometric replication model, smaller f_r will decrease cusp spacing for the same radius R thus lowering Sa. Increasing R does not change the cusp spacing but changes the cusp height, again reducing Sa. Target values for Sa are in the range of 1 nm to 2 nm (or better) for visible light applications and on the order of 30 nm for infrared applications. Since there are practical and cost limits to increasing R (e.g., larger diamonds, limiting inventory, etc.), decreasing f_r is the primary option for meeting a roughness specification. However, reducing f_r linearly increases machining time, introducing other problems, and cost. The goal is to machine an optic as fast as possible while meeting the necessary surface finish specification by minimizing the time for changes in other parameters, such as temperature, that cause issues such as form and mid-spatial frequency errors.

The parameter ranges chosen for training the machine learning model are given in Table 1. It was expected that for low f_r (< 1 nm) and for high f_r (> 20 nm) the measured Sa will deviate from the simple geometric model. Under these conditions, the effects of other parameters become important and these dependencies can be identified by the machine learning model. Thus, it may be possible to use the machine learning model to suggest new hypotheses about the physics of the diamond machining process.

MACHINE LEARNING MODEL

In recent years, the growth in data availability and computational power, coupled with advances in data learning modeling approaches, has led to broader uses of machine learning techniques and has shown increased success in solving highly complex tasks, such as image object identification, voice recognition, and self-driving cars. Supervised machine learning algorithms approximate a nonlinear function by mapping, or modeling, the

[a] The rake angle is the angle between the tool front face and the line perpendicular to the surface being machined.
[b] The axial depth of cut is the depth of tool penetration into the initial surface.
[c] The feed per revolution is the motion of the tool per revolution of the workpiece given by $f_r = V_f/\Omega$.

relationships between input(s) and corresponding output(s) guided by input-output pairs of observation measurements of a system. This is the "model training" phase of the machine learning process. In a subsequent "model testing" (simulation) phase, the model can then be used for predicting output values of the function when provided with new input data. For this work, input parameter values listed in Table 1 define the diamond turning process that was used to collect 78 measurements of the resulting surface roughness Sa. The set of 78 input-output pairs constitutes the dataset used for experiments with two traditional machine learning regression algorithms, Support Vector Machine (SVM) and Gaussian Process Regression (GPR) models, as well as a Generalized Regression Neural Network (GRNN).

A GRNN is a one-pass neural network algorithm that provides estimates for continuous dependent variables and converges to the (underlying) regression surface [17]. This artificial neural network has several advantages in comparison to other nonlinear regression modeling techniques, including fast learning, generalization from sample examples, insensitivity to the local minima problem, and consistent convergence to global solutions.

There are two reasons for selecting a GRNN to predict surface roughness. First, this type of network is capable of producing reliable predictions even with a small observation set for model training. The prohibitive cost of collecting a large number of sample measurements from ultra-precision diamond turning experiments makes GRNNs an appropriate choice. Second, a GRNN is capable of handling noise within the inputs. The observation samples are inherently noisy in this domain. Surface roughness is a function of many parameters which are connected only indirectly to the measured input parameters: high strain rate thermo-plastic material flow, vibrations, environmental temperature fluctuations, and other factors. These dependencies are more pronounced for very low and high f_r values.

The overall architecture of the implemented GRNN is shown in Figure 2. The GRNN is a two-layer network similar to a radial basis function network, but with a slightly different second layer. As shown, the GRNN network has a highly parallel structure and implements a one-pass learning algorithm that does not require an iterative training procedure as in back propagation [17]. The input for the network is formed with nodes in equal number to the independent input parameters to be modeled. The machining parameter values are fed to the GRNN via the input nodes that provide these values to each neuron[d] in the radial basis (hidden) layer. The first (hidden) layer comprises nonlinear radial basis neurons with as many neurons as the number of sample observations available for training, i.e., 78 neurons for the 78 experiments. Each neuron in the first (hidden) layer is associated with only one of the sample observations and stores its corresponding dependent output parameter, Sa. Similar to biological neurons, each neuron in the neural network receives one or more inputs from the previous layer, performs a mathematical transformation on these values and sends the results to the next layer. The special linear layer has purelin transfer function neurons equal to the number of sample observations, i.e., 78, and the number of neurons in the first layer. This second layer computes a weighted function of the values received from the first layer and uses a linear transfer function to determine the second layer's output which is sent to the output node. The value of the output node corresponds to the surface roughness predicted value.

[d] An artificial neuron is a mathematical function conceived as a model of the biological neuron in the brain. Neurons are the basic units typically used to build artificial neural networks (ANN). A neuron receives input values, processes and passes them to the next layer of the network. ANNs simulate the network of neurons in the human brain and are capable of learning from data and making decisions in a human-like manner.

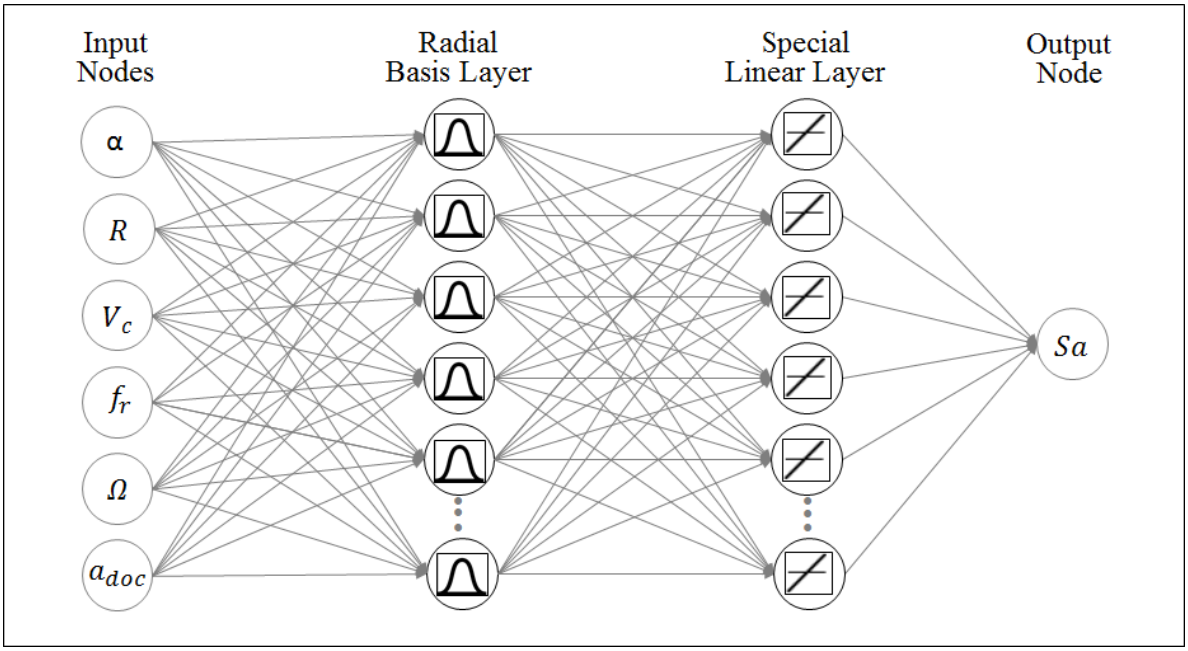

Figure 2: Generalized regression neural network architecture

For brevity, a detailed explanation of the GRNN inner-workings is not provided here, but it is important to mention that the GRNN has only one unknown, free parameter, the *spread* constant σ. The radial basis layer computes bias as a constant 0.8326/*spread.* Thus, the spread controls the area around the input parameters and affects the radial basis function's slope in the first layer neurons. Larger *spread* values produce a smoother slope causing more neurons in the network to respond to the input parameters, thus increasing their contribution to the weighted output. The result is that the network approximates the input parameter values to the output value associated with the training set of input parameters closest to the new input parameters. A main disadvantage of the GRNN is that their size grows very quickly with the number of input sample observations used for training, thus rendering large networks computationally intensive. This is not a concern for this work, however, because the high cost of obtaining experimental data limits the size of the training dataset.

RESULTS

Prior to applying the data learning model to the experimental data, a set of computational experiments with different sets of input parameters, or input vectors, was developed. For example, one input vector consisted of parameters: Ω, V_c, a_{doc}, and f_r, while another consisted only of V_c, a_{doc}, and f_r, etc. Using the MATLAB R2018b Statistics and Machine Learning Toolbox™, 19 traditional regression machine learning algorithms (e.g., SVM, GRP) were trained for each set of input vectors to evaluate the available data and obtain insights about individual machining parameters and how their behavior, together and separately, affect surface roughness outcomes. Since the input machining parameters have various units and ranges, a best practice is to scale the data to a common notional scale. In this case, the data was normalized to have "unit" standard deviation and zero mean. The input parameters in our sample dataset with invariant values, tool nose radius R and rake angle α, have zero standard deviation and were removed from the dataset. Next, the 78 normalized inputs and their associated output values were split into training and testing sets using a five-fold cross-validation strategy. For each input parameter vector tested, the model with the smallest root-mean-square error (RMSE) was selected as the best model among the 19 models generated. Table 2 describes the four input parameter vectors tested, the best model found, and its corresponding RMSE results. These initial models provided a basis for analysis of the behavior of the machining data features/parameters.

Table 2: Traditional regression machine learning algorithm results

Experiment	Input Parameter Vector	Selected Best Model	RMSE
1	$V_c, f_r, \Omega, a_{doc}$	Squared Exponential GPR	5.8344
2	f_r, Ω, a_{doc}	Quadratic SVM	5.2207
3	f_r, Ω	Squared Exponential GPR	4.7141
4	f_r	Squared Exponential GPR	3.7359

The GRNN model was implemented using the MATLAB R2018b Deep Learning Toolbox™. A GRNN was trained using the 78 input-output experimental dataset, where the input vector parameters consisted of the four machining parameters listed in Experiment 1 of Table 2 and *spread* equal to 0.7. For a true blind test of the GRNN model, 20 new sample values of the input parameters were selected—never seen before by the neural network and for which the corresponding surface roughness had not being measured—which were then fed to the GRNN model to obtain a resultant Sa prediction. Figure 3 illustrates the Sa results obtained with the GRNN model.

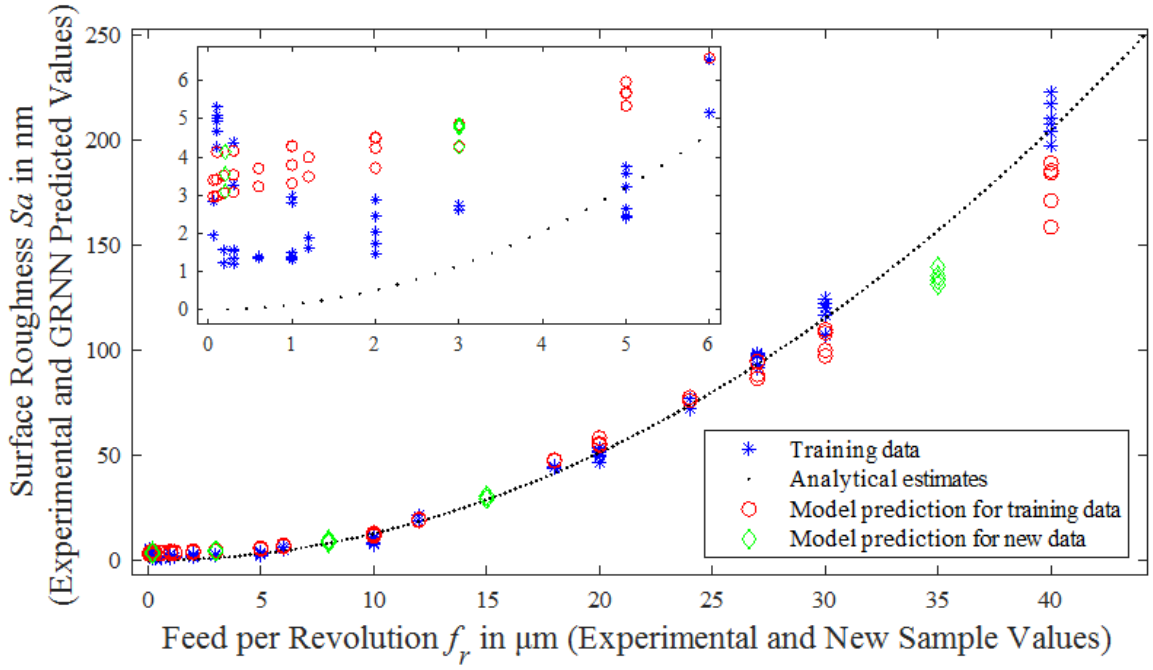

Figure 3: Plots of the experimental results, the geometric analytical model, and the predicted results of the machine learning model.

Figure 3 shows four different sets of results. Data points labeled “training data” correspond to the original 78 input-output sample observations used for training the model. Equation 1 was used to calculate “analytical estimates” of Sa for all values within the f_r range resulting in the smooth dotted curve. Once the model was trained, the original 78 input sample observations were fed to the model to obtain “model predictions for the training data” and the 20 new sample values of the input parameters for the blind test to produce the “model prediction for the new data” data points. The inset overlaid on Figure 3 shows in detail the resulting Sa for the lower f_r range.

Figure 4 provides a comparison of the measured and predicted values of Sa for the GRNN model, where the input vector parameters consisted of the four machining parameters listed in Experiment 1 of Table 2 and *spread* equal to 0.7. While Figure 3 plots Sa against only one of the input parameters, the feed per revolution f_r, Figure 4 captures the collective influence of all four machining parameters in assessing the predictive performance of the GRNN model.

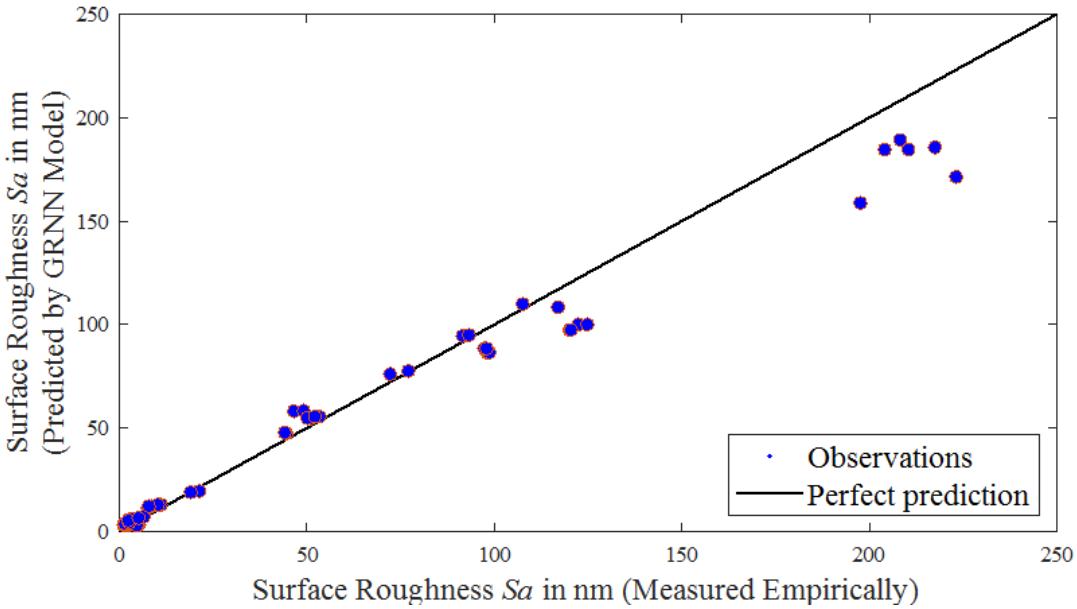

Figure 4: Comparison of measured and predicted surface roughness

DISCUSSION

The training data plotted in Figure 3 generally follows the analytical (geometric) curve. However, it diverges from the analytical estimate for lower values of f_r, which, as discussed earlier, may be due to more complex material flow effects, thermal fluctuations, or other physical phenomena. Both data learning models mimic the increased roughness at lower feed rates. The GRNN predictions that appear well below the analytical estimate at higher feed rates are physically impossible. While some deviation below the estimation curve can occur due to rounding of cusps peaks, it is unclear what parameter is driving the model down. The predictions produced in the middle range of f_r agree with the analytical and training data. This provides insight and motivation that the models need to incorporate the more complex effects that occur during the cutting operation. Figure 4 also indicates three sub-regions of performance. At the higher values of Sa, predicted values of Sa fall significantly below measured values, while at the lower values of Sa, the predicted values of Sa fall slightly above measured values.

CONCLUSIONS

This work introduces a general regression neural network (GRNN) model for estimating the surface roughness Sa of an ultra-precision diamond turning process in OFHC copper. The model input consists of the spindle speed or rotation rate Ω in rev/min (rpm), tool nose radius R in µm, rake angle α in degrees, cutting speed V_c in m/s, feed velocity V_f in mm/min, axial depth of cut a_{doc} in µm, and feed per revolution f_r in µm. The Sa values predicted by the GRNN model are compared to experimental data collected in laboratory tests and Sa data calculated using the analytical (geometric) model defined by Eq. 1. The GRNN model was able to generalize the training dataset results to a new dataset not utilized during the network training.

This is a first step to demonstrate the feasibility of using ANNs for determining the surface finish of diamond turning processes. The simulation results obtained with the GRNN model are encouraging as it significantly outperformed the analytical model estimates on the lower end of the inputs' range. Of particular interest for further study are the three sub-regions of model performance across the spectrum of feed per revolution f_r. Current results suggest that aspects of high-strain rate material flow, among other factors, may not be adequately reflected in the current model, especially in regions of low surface roughness. Next steps include the implementation of physics-guided ANNs that are able to improve model performance to conform with physical constraints. At the higher regions of surface roughness, physics-guided ANNs are able to penalize the model for predictions below the geometric limit. Further experiments with other complex materials will be conducted to both confirm the superior performance of the GRNN model and validate the complex behaviors observed across the spectrum of feed per revolution. To supplement the training data we will be using machining simulation data in addition to experiments. Further, the ANN model will be augmented with physical

models that, for example, penalize predictions that are below the geometric prediction and are thus physically not possible.

Finally, the machining operation considered here is quite well behaved in that it follows the geometric model over a wide range of parameters fairly closely. Particularly for applications in infrared optics which must be manufactured in brittle materials, the material behavior is much more complex. For these more complex situations, a machine learning model that predict the most productive machining parameters that meet the specifications is of great practical benefit.

References

[1] Rhorer, R., Evans, C. (1995) Handbook of Optics – Fabrication of Optics by Diamond Turning; Chapter 41. McGraw-Hill.

[2] Zhang, H., Zhang, X. (1994) Factors affecting surfaces quality in diamond turning of oxygen-free high-conductance copper"; Applied Optics, 33(10):2039-2042. doi: 10.1364/AO.33.002039.

[3] Davies, M.A., Owen, J.D., Troutman, J.R., Barnhardt, D.L., Suleski, T.J. (2015) Ultra-precision diamond machining of freeform optics, 2015, Imaging and Applied Optics 2015, OSA Technical Digest (online) (Optical Society of America, 2015), paper FM1B.1, doi:10.1364/FREEFORM.2015.FM1B.1.

[4] Shultz, J.A., Davies M.A., Suleski, T.J. (2015) Effects of MSF errors on performance of freeform optics: Comparison of diamond turning and diamond milling, Imaging and Applied Optics 2015, OSA Technical Digest (online) (Optical Society of America), paper FT4B.3.

[5] Thompson, A.K. (1998) Scattering effects of machined optical surfaces. Source DAI-B 59/03, UMI, 151 pages.

[6] Taylor, J.S., Syn, C.K., Saito, T.T., Donaldson, R.R. (1986) Surface Finish Measurements Of Diamond-Turned Electroless-Nickel-Plated Mirrors. Large Optics Technology Proc. SPIE 0571. 25(9) 251013. https://doi.org/10.1117/12.950369.

[7] Owen, J.D., Troutman, J.R., Harriman, T.A,. Zare, A., Wang, Y.Q., Lucca, D.A., Davies, M.A. (2016) The mechanics of milling of germanium for IR applications. CIRP Annals - Manufacturing Technology, 65(1):109-113.

[8] Özel T., Karpat Y. (2005) Predictive modeling of surface roughness and tool wear in hard turning using regression and neural networks. Intl Jour of Machine Tools and Manufacture, 45(4–5):467-479. https://doi.org/10.1016/j.ijmachtools.2004.09.007.

[9] S.K Choudhury, G Bartarya, Role of temperature and surface finish in predicting tool wear using neural network and design of experiments, Intl Jour of Machine Tools and Manufacture, 43(7):747-753, 2003, https://doi.org/10.1016/S0890-6955(02)00166-9.

[10] Liang, S.Y., Hecker, R.L., Landers, R.G. (2002) Machining Process Monitoring and Control: The State–of–the–Art. ASME International Mechanical Engineering Congress and Exposition, Manufacturing 599-610. doi:10.1115/IMECE2002-32640.

[11] Paturi, U.M.R., Devarasetti, H., Narala, S.K.R. (2018) Application of Regression and Artificial Neural Network Analysis Modeling of Surface Roughness in Hard Turing of AISI 52100 Steel. Materials Today, Proceedings, 5:4766-4777. https://doi.org/10.1016/j.matpr.2017.12.050

[12] Wang, X., Feng, C.X. (2002) Development of Empirical Models for Surface Roughness Prediction in Finish Turning, Int J Advanced Manufacturing Technology, 20(5): 348–356.

[13] Petropoulos, G., Mata, F,, Davim, J.P. (2008) Statistical study of surface roughness in turning of peek composites. Materials and Design, 29(1):281-223.

[14] Muthukrishnan, K., Davim, J.P. (2009) Optimization of machining parameters of Al/SiC-MMC with ANOVA and ANN analysis. Jour Materials Processing Technology, 209(1): 225-232. https://doi.org/10.1016/j.jmatprotec.2008.01.041.

[15] Palanikumar, K., Karthikeyan, R. (2007) Optimal Machining Conditions for Turning of Particulate Metal Matrix Composites Using Taguchi and Response Surface Methodologies, Machining Science and Technology. 10(4): 717-433. https://doi.org/10.1080/10910340600996068.

[16] Gupta, M. Kumar, S. (2015) Investigation of surface roughness and MRR for turning of UD-GFRP using PCA and Taguchi method. Engineering and Science Technology: An International Journal. 18(1):70-81. https://doi.org/10.1016/j.jestch.2014.09.006.

[17] Specht, D.F. (1991) A general regression neural network. IEEE Transactions on Neural Networks, 2(6): 568-576.